Lithium and Cesium Ion-Pair Acidities of Diphenylamine in Tetrahydrofuran. The Aggregation of Lithium and Cesium Diphenylamide. A New Method for the Determination of Aggregation Constants in Dilute Solution[1]

James A. Krom, Jeffrey T. Petty, and Andrew Streitwieser*

Contribution from the College of Chemistry, University of California, Berkeley, California 94720

Received March 1, 1993

Abstract: An investigation of the aggregation of lithium and cesium diphenylamide (LiDPA and CsDPA, respectively) in tetrahydrofuan solution has been carried out. Two independent methods were used; one makes use of the effect of concentration in the observed ion-pair acidity of diphenylamine, and the other is based on a spectral analysis. LiDPA is found to be a monomeric contact ion pair, in agreement with Collum's NMR results. For CsDPA, the two methods yield results that are in agreement only if a monomer/dimer equilibrium is assumed. All other hypotheses can be ruled out with high confidence. At 25 °C, the dimerization constant is found to be 160 ± 10 M^{-1}. Together with experiments conducted at −15 °C, we find the thermodynamics of dimerization to be approximately $\Delta H° = -2$ kcal/mol and $\Delta S° = 4$ eu. At 25 °C, the lithium and cesium ion-pair pKs of diphenylamine are 19.05 and 24.20, respectively.

Ions, ion pairs, and ionic aggregates derived from organic substrates are key intermediates in many chemical reactions. Consequently, many studies have been carried out in order to elucidate those factors that govern their structures and reactivities.[2] Much of the attention has focused on lithium amides[3] because of their importance in synthetic applications, and several general structural features have emerged. Lithium amides typically crystallize as polymeric aggregates in the absence of donating solvents, with rings composed of alternating lithium and nitrogen atoms being a common structural motif.[3] In the presence of donating ligands, they generally crystallize as monomeric or dimeric species. In solution, the degree of aggregation is often similar to that observed in the solid state but sometimes, measurable equilibria among species are observed.[3] For example, lithium hexamethyldisilazide (LHMDS) crystallizes as a trimer from petroleum ether,[4] but in tetrahydrofuran (THF) and hydrocarbon solvents, it exists as a mixture of monomers/dimers and dimers/tetramers, respectively.[5] A study on the structure and reactivity of lithium diisopropylamide (LDA) showed that LDA in THF is essentially dimeric, but the kinetics of reaction suggest that the monomeric species is the actual reactive intermediate in the metalation of a hydrazone.[6,7]

Clearly, the degree of aggregation of a solute depends on the energetics of solvent–solute interactions compared to those of solute–solute interactions.[8] Restricting the discussion to a given anion, the relative importance of these interactions is affected by variables such as solvent, concentration, temperature, and cation. As the examples cited above point out, a detailed understanding of the influence of these variables is essential in interpreting reactivity. We are especially interested in the influence of the cation on acidity, aggregation, and reactivity.

There is scant information available regarding the effect of heavier alkali cations on the aggregation of amides. The alkali derivatives of hexamethyldisilazane are the most extensively studied;[9] the sodium salt[10] is polymeric in the crystal, while the potassium salt crystallizes from toluene as a dimer with two coordinating solvent molecules.[11] The crystal structures of some aromatic amides of the heavier alkali metals have been determined[12] and show a tendency for these compounds to form dimeric species. Finally, NMR results suggest that the tetramethylethylenediamine (TMEDA) adduct of *N*-sodioindole is dimeric in toluene.[12]

In this study, we make use of two independent methods in order to investigate the aggregation of lithium and cesium diphenylamide (LiDPA and CsDPA, respectively) in THF solution. One method makes use of the recently developed cesium ion-pair acidity scale,[13] and the other relies on a detailed analysis of the UV–visible absorption spectrum of CsDPA. We show that neither method alone is capable of providing compelling evidence regarding the nature of the aggregates that are in solution but, taken together, the data are consistent with only one aggregation model. The results are also consistent with Collum's findings for LiDPA.[14]

Results

All of the experiments were carried out in THF solution at 25.0 °C, unless otherwise stated.

UV–Visible Absorption Spectra. The absorption spectrum of LiDPA was found to have a λ_{max} of 351.5 nm with an extinction coefficient of 24 000 ± 500 M^{-1} cm^{-1}. The shape of the absorption band was independent of concentration.

The shape of the absorption band of CsDPA was found to be concentration-dependent: the λ_{max} gradually shifted from 369 to 367 nm as the formal concentration was increased incrementally

(1) Carbon Acidity. 86.
(2) *Ions and Ion Pairs in Organic Reactions*; Szwarc, M., Ed.; Wiley: New York, 1972.
(3) For review, see: Gregory, K.; Schleyer, P. v. R.; Snaith, R. *Adv. Inorg. Chem.* **1991**, *37*, 47.
(4) Mootz, D.; Zinnius, A.; Böttcher, B. *Angew. Chem., Int. Ed. Engl.* **1969**, *8*, 378.
(5) Kimura, B. Y.; Brown, T. L. *J. Organomet. Chem.* **1971**, *26*, 57.
(6) Galiano-Roth, A. S.; Collum, D. B. *J. Am. Chem. Soc.* **1989**, *111*, 6772.
(7) For many other examples, see ref 3.
(8) *Solute–Solvent Interactions*; Coetzee, J. F., Ritchie, C. D., Eds.; Marcel Dekker: New York, 1969.
(9) Lappert, M. F.; Power, P. P.; Sanger, A. R.; Srivastava, R. C. *Metal and Metalloid Amides*; Ellis Horwood: Chichester, 1980.
(10) Grüning, R.; Atwood, J. L.; *J. Organomet. Chem.* **1977**, *137*, 101.
(11) Williard, P. G. *Acta Crystallogr., Sect. C: Cryst. Struct. Commun.* **1988**, *C44*, 270.
(12) (a) Gregory, K.; Bremer, M.; Schleyer, P. v. R.; Klusener, P. A. A.; Brandsma, L. *Angew. Chem.* **1989**, *101*, 1261. *Angew. Chem., Int. Ed. Engl.* **1989**, *28*, 1224. (b) Gregory, K.; Bremer, M.; Bauer, W.; Schleyer, P. v. R. *Organometallics* **1990**, *9*, 1485.
(13) (a) Streitwieser, A.; Ciula, J. C.; Krom, J. A.; Thiele, G. *J. Org. Chem.* **1991**, *56*, 1074. (b) Kaufman, M. J.; Gronert, S.; Streitwieser, A., Jr. *J. Am. Chem. Soc.* **1988**, *110*, 2829. (c) Bors, D. A.; Kaufman, M. J.; Streitwieser, A., Jr. *J. Am. Chem. Soc.* **1985**, *107*, 6975. (d) Streitwieser, A., Jr.; Bors, D. A.; Kaufman, M. J. *J. Chem. Soc., Chem. Commun.* **1983**, 1394.
(14) DePue, J. S.; Collum, D. B. *J. Am. Chem. Soc.* **1988**, *110*, 5518.

0002-7863/93/1515-8024$04.00/0

from about 1×10^{-4} to about 5×10^{-4} M. However, the observed extinction coefficient at 367 nm was concentration-independent to within the experimental error and was found to be 28 800 ± 400 M^{-1} cm^{-1}. The stated uncertainty is the standard deviation of five determinations. At −15.0 °C, the shape of the absorption band was found to be similarly concentration-dependent, with a constant extinction coefficient of 30 100 ± 100 M^{-1} cm^{-1} at 368 nm.

In our treatment of the absorption data for CsDPA, we made use of the linear-algebraic method "singular-value decomposition" (SVD).[15] Briefly, SVD is a linear-algebraic method that decomposes an input matrix **B** into three new matrices according to the equation $\mathbf{B} = \mathbf{USV}^t$, where **U** is a matrix containing an orthonormal basis for the column vector space of **B**, **V** is an orthonormal matrix, and **S** is a diagonal matrix containing the so-called singular values. $\mathbf{V}^t$ denotes the transpose of **V**. The singular values are "weighting factors" for the associated vectors in **U**; the larger the singular value, the more important the associated vector in **U** is in describing the original set of vectors **B**. It is important to note that the vectors of **U** are not chemically meaningful spectra but are orthonormal basis vectors that best describe the observed spectra in a least-squares sense.[15] In method B, described below, we find a linear transformation of the vectors of **U** into meaningful spectra for each species in solution.

We used SVD to process a set of 12 absorption spectra of CsDPA at 25.0 °C, each obtained at a different formal concentration. The absorbance data were collected at 0.5-nm intervals over the range of 340.0–450.0 nm. Thus, the matrix **B** consisted of 221 rows and 12 columns, each column corresponding to an absorption spectrum. SVD gave 12 singular values, the largest two having the values $S_1 = 28.10$ and $S_2 = 0.34$; the other singular values fell between 8.82×10^{-3} and 3.05×10^{-2}. To within the noise of the spectrophotometer, the appropriate linear combinations of the two columns of **U** (denoted U_1 and U_2, respectively) corresponding to the singular values S_1 and S_2 were adequate to describe the original set of data; the remaining columns describe the noise, that is, we can model the variable spectrum of CsDPA with the appropriate linear combination of U_1 and U_2. Assuming that the absorbances of all chemical species obey Beer's law, we can conclude that there are only two spectroscopically distinguishable species in solution, their relative concentrations being a function of the formal (total) concentration.

Similarly, for a series of 10 absorption spectra obtained at −15.0 °C, SVD again showed that two functions were adequate to describe the data, with singular values 29.93 and 0.38.

Ion-Pair Acidity. The lithium ion-pair acidity[13b,16] of DPA was measured against the indicator 9-phenylfluorene (PhFL, $pK_{Li} = 17.60$). In acidity experiments, we determined the concentrations of the ion pairs by fitting the separate UV–visible spectra of the indicator ion pair and the substrate ion pair to the equilibrium spectrum (the "double indicator" method; see the Experimental Section). The results are shown in Table I. The dissociation of the lithiated 9-PhFL (LiPhFL) to the free ions causes a slight but significant dependence of the observed equilibrium constant (eq 1a) on the formal concentration of LiPhFL. The known[13b] dissociation constant of LiPhFL allows

$$\text{LiPhFL} + \text{DPA} \rightleftharpoons \text{PhFL} + \text{LiDPA} \qquad (1a)$$

the appropriate correction to be applied to the experimental data; the corrected ion-pair equilibrium constants are shown in the last column of Table I. It is clear that the corrected equilibrium constants do not vary with the concentration of LiDPA, and we can conclude that LiDPA is not significantly aggregated at these concentrations (see below).

Table I. Lithium Ion-Pair Acidity of DPA against PhFL in THF at 25.0 °C

$$\text{LiPhFL} + \text{DPA} \rightleftharpoons \text{PhFL} + \text{LiDPA}$$

{LiDPA} (10^{-5} M)	{LiPhFL} (10^{-4} M)	DPA (10^{-3} M)	PhFL (10^{-3} M)	$10^2 \times K_{ob}$	$10^2 \times K_{corr}$[a]
2.17	1.53	1.468	2.919	2.82	3.64
2.83	1.91	1.809	3.596	2.95	3.70
3.64	2.44	2.285	4.539	2.97	3.63
15.42	2.48	2.421	1.116	2.87	3.50
18.78	2.73	5.485	2.342	2.94	3.56
17.77	2.83	2.750	1.267	2.90	3.50
1.82	2.90	1.318	6.516	3.11	3.74
4.57	3.03	2.784	5.524	3.00	3.60
4.74	3.21	2.869	5.723	2.94	3.51
20.92	3.25	3.174	1.464	2.97	3.54
23.39	3.33	6.690	2.856	3.00	3.57
23.22	3.61	3.511	1.617	2.96	3.50
5.67	3.70	3.366	6.675	3.03	3.58
2.24	3.77	1.632	8.066	2.94	3.47
5.98	3.88	3.436	6.850	3.07	3.61
29.16	4.09	8.211	3.506	3.05	3.56
2.70	4.22	1.888	9.328	3.16	3.69
34.02	4.73	9.439	4.027	3.07	3.55
7.69	4.92	4.314	8.596	3.11	3.59
3.16	4.95	2.189	10.81	3.15	3.63
40.63	5.58	11.09	4.729	3.10	3.55
9.14	5.81	5.037	10.03	3.13	3.57
3.87	5.95	2.600	12.84	3.21	3.66
4.09	6.73	2.880	14.20	3.00	3.38
12.01	7.56	6.404	12.74	3.16	3.55
59.20	7.85	15.39	6.553	3.21	3.59

[a] Corrected for the dissociation of LiPhFL to free ions.

Table II. Observed Cesium Ion-Pair Acidity of DPA against *t*-BuFL in THF at 25.0 °C

$$\text{Cs-}t\text{-BuFL} + \text{DPA} \rightleftharpoons t\text{-BuFL} + \text{CsDPA}$$

{CsDPA} (10^{-4} M)	Cs-*t*-BuFL (10^{-4} M)	DPA (10^{-2} M)	*t*-BuFL (10^{-2} M)	K_{ob}
0.23	0.67	0.779	3.327	1.47
0.48	1.25	0.777	3.321	1.63
0.52	0.49	1.211	1.816	1.60
0.76	2.05	0.774	3.314	1.59
1.01	2.73	0.771	3.307	1.58
1.33	3.54	0.768	3.299	1.61
1.46	1.34	1.201	1.808	1.64
1.62	4.31	0.765	3.291	1.62
2.03	5.39	0.761	3.280	1.62
2.25	2.03	1.194	1.801	1.67
2.51	6.54	0.756	3.269	1.66
2.79	1.26	1.427	1.105	1.71
2.82	2.50	1.188	1.796	1.70
3.05	7.77	0.751	3.256	1.70
3.69	3.27	1.179	1.788	1.71
3.83	1.72	1.417	1.101	1.73
4.61	3.97	1.170	1.781	1.77
4.72	2.08	1.408	1.097	1.77
5.56	4.68	1.160	1.774	1.82

The cesium ion-pair acidity[13] of DPA was measured against the indicator 9-*tert*-butylfluorene (*t*-BuFL, $pK_{Cs} = 24.39$). In the present case, it was necessary to account for the concentration dependence of the spectrum of CsDPA; therefore, we used U_1, U_2, and the spectrum of Cs-*t*-BuFL to deconvolute the equilibrium spectra. The spectrum (and therefore the concentration) of

$$\text{Cs-}t\text{-BuFL} + \text{DPA} \rightleftharpoons t\text{-BuFL} + \text{CsDPA} \qquad (1b)$$

CsDPA was then determined from the combination of U_1 and U_2. The acidity results are presented in Table II. The dependence of the observed equilibrium constant (eq 1b) of DPA on the formal

(15) (a) Golub, G. H.; Reinsch, C. In *Linear Algebra*; Wilkinson, J. H., Reinsch, C., Eds.; Springer–Verlag: Heidelberg, 1971, and references therein. (b) Press, W. H.; Flannery, B. P.; Teukolsky, S. A.; Vetterling, W. T. *Numerical Recipes (Fortran Version)*; University Press: Cambridge, 1989. (c) Malinowsky, E. R. *Factor Analysis in Chemistry*; Wiley: New York, 1991.

(16) Gronert, S.; Streitwieser, A., Jr. *J. Am. Chem. Soc.* **1986**, *108*, 7016.

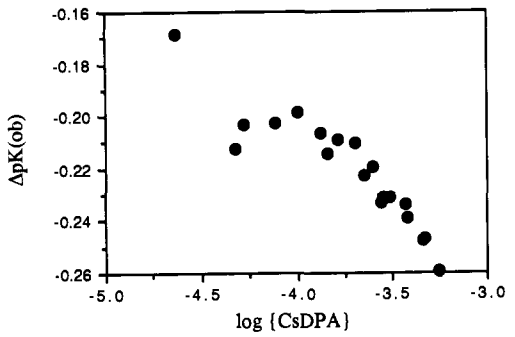

Figure 1. Aggregation plot for CsDPA. There is a large degree of scatter in the data because the errors are experimentally correlated between the variables.

concentration of CsDPA indicates that aggregation of CsDPA is significant. Figure 1 shows the plot of pK_{ob} vs log {CsDPA} (the braces denote formal concentration); it has been shown[17] that the slope of the plot is equal to $(1/\bar{n}) - 1$, where $\bar{n}$ is the average aggregation number. At the lowest concentrations, CsDPA is essentially monomeric, but at the highest concentrations, the slope gives $\bar{n} = 1.1$. The cesium ion-pair acidity of DPA was also obtained at −15 °C, and the data again showed that CsDPA is aggregated at this temperature, with an average aggregation number of about 1.1.

The results of the SVD analysis for CsDPA imply that there are at least two distinct species in solution; we shall now assume that there are exactly two, and from the acidity interpretation, we have concluded that they are ion-pair aggregates. It is clear from the acidity results that the monomeric ion pair is present, and we desire to obtain evidence regarding the stoichiometry of the other. We do so by comparing the results obtained from two independent analyses of the data.

Method A. The method is an analysis of the ion-pair acidity data. The formal ion-pair concentration is given by

$$\{\text{CsDPA}\} = \sum_n n[(\text{CsDPA})_n] = \sum_n nK_n[(\text{CsDPA})_1]^n \quad (2)$$

where $[(\text{CsDPA})_n]$ is the molar concentration of the aggregate composed of n ion pairs and K_n is the equilibrium constant for the reaction

$$n(\text{CsDPA})_1 \rightleftharpoons (\text{CsDPA})_n \quad (3)$$

Furthermore, the observed acidity with respect to the indicator t-BuFL is given by

$$K_{ob} = \frac{\{\text{CsDPA}\}[t\text{-BuFL}]}{[\text{DPA}][\text{Cs-}t\text{-BuFL}]} = K_a\frac{\{\text{CsDPA}\}}{[(\text{CsDPA})_1]} \quad (4)$$

where K_a is the true cesium ion-pair acidity constant of DPA relative to the indicator. Solving (4) for {CsDPA} and substituting into (2) gives

$$\{\text{CsDPA}\} = \sum_n nK_nK_a^n(\{\text{CsDPA}\}/K_{ob})^n \quad (5)$$

Equation 5 is a polynomial in the known quantity $\{\text{CsDPA}\}/K_{ob}$; by plotting {CsDPA} against $\{\text{CsDPA}\}/K_{ob}$ and fitting a polynomial to the data, K_a and K_ns can be determined. The polynomial to be fit is based on the underlying hypothetical model for the chemical system. For example, if we assume a monomer/dimer equilibrium, the equation takes the form $y = a_1x + a_2x^2$, where the coefficients are the adjustable parameters for the fitting.

The plot of {CsDPA} vs $\{\text{CsDPA}\}/K_{ob}$ is shown in Figure 2; the data are taken from Table II. Polynomials corresponding to the hypotheses monomer/dimer, monomer/trimer, and monomer/tetramer were fit to the experimental data. The results of the least-squares fits are presented in Table III. The data do not allow us to reject any of the hypotheses, that is, each of the polynomials fits the data to within the experimental precision but different equilibrium constants are obtained for each hypothesis.

(17) Kaufman, M. J.; Streitwieser, A., Jr. *J. Am. Chem. Soc.* **1987**, *109*, 6092.

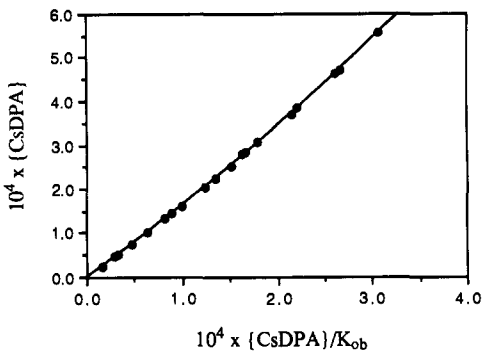

Figure 2. Determination of the equilibrium constants at 25 °C by method A. The line is the best fit of eq 5 to the experimental data (see Table III). The data are taken from Table II.

Table III. Aggregate Equilibria Calculated According to Method A

$$n(\text{Cs-DPA}) \overset{K_n}{\rightleftharpoons} (\text{Cs-DPA})_n$$

hypothesis, n	a_1[a,c]	a_n[a,c]	K_n[b,c]
2	1.54 ± 0.08	870 ± 130	180 ± 20 M^{-1}
3	1.62 ± 0.09	(2.1 ± 0.2) × 10^6	(1.7 ± 0.2) × 10^5 M^{-2}
4	1.65 ± 0.09	(6.2 ± 0.7) × 10^9	(2.1 ± 0.3) × 10^8 M^{-3}

[a] These are the adjusted parameters found by least-squares fit to eq 5. $a_1 = K_a$, the true cesium ion-pair acidity constant, and $a_n = nK_nK_a^n$. The plot of the data is shown in Figure 2. [b] Calculated from the adjusted parameters according to eq 5. [c] The uncertainties are one standard deviation, including both systematic and random error analysis. See the Experimental Section for details.

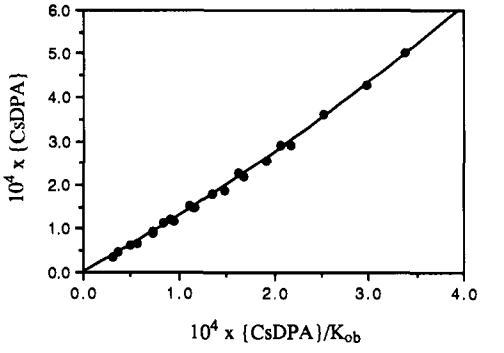

Figure 3. Determination of the equilibrium constants at −15 °C by method A. The line is the best fit of eq 4 to the experimental data, assuming a monomer/dimer equilibrium.

Cesium ion-pair acidity data were also obtained at −15 °C; the plot of {CsDPA} vs $\{\text{CsDPA}\}/K_{ob}$ is shown in Figure 3. Assuming a monomer/dimer equilibrium (see Discussion section), the least-squares fit of the equation $y = ax + bx^2$ gives $a = 1.21 \pm 0.03$ and $b = 770 \pm 150$ and from eq 5, $K_2 = 260 \pm 50$ M^{-1}.

Method B. This method is an analysis of the absorption spectrum of CsDPA as a function of concentration and utilizes the SVD output; the mathematical details are relegated to the Appendix. It is essentially a factor analysis.[15c] The goal is to find the spectrum and extinction coefficients of each of the aggregates in solution and thereby determine the equilibrium constants among them. Of course, we do not know which species (monomer and dimer, etc.) are actually present, so we calculate the results for a series of hypothetical mixtures. For example, if we assume that the mixture consists of monomers and dimers, from the equilibrium between them, the absorbance of the dimer

Table IV. Spectral Data and Equilibrium Constants Calculated According to Method B

hypothesis, n	ϵ_1[a,e]	$\lambda_{max}(CsDPA)_n$[b]	$\epsilon_{367}(CsDPA)_n$[c,e]	K_n[d,e]
2	28 800 ± 400	352.0	57 500 ± 1500	144 ± 7 M^{-1}
3	28 800 ± 400	357.5	86 300 ± 800	(9.3 ± 0.3) × 10^5 M^{-2}
4	28 800 ± 400	365.0	115 400 ± 1000	(3.0 ± 0.2) × 10^9 M^{-3}

[a] Extinction coefficient of the hypothetical monomer at 367 nm, in M^{-1} cm^{-1}. The calculated λ_{max} was 369.5 nm in every case. [b] λ_{max} of the hypothetical aggregate of degree n, in nm. [c] Extinction coefficient of the hypothetical aggregate at 367 nm, in M^{-1} cm^{-1}. [d] Equilibrium constant for eq 3 in the text. [e] The uncertainties are one standard deviation, including random and systematic error analysis. See the Experimental Section for details.

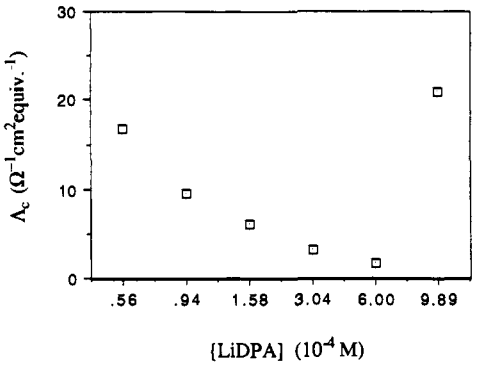

Figure 4. Plot of equivalent conductance vs concentration of LiDPA in THF at 25.00 ± 0.04 °C.

at each wavelength must be proportional to the square of the absorbance of the monomer. Under this constraint, we can find the spectra of the monomer and dimer and calculate the equilibrium constant. We repeat this procedure for all hypotheses (monomer/trimer, etc.), and, in general, none of the hypotheses can be ruled out.

The SVD output was processed according to this method; for the reasons discussed previously, we again used only the columns of U and the rows of V^t associated with the two largest singular values S_1 and S_2. The relevant spectral data and equilibrium constants are collected in Table IV. The tabulated aggregation constants are the averages of the values found from the spectra obtained at the eight highest formal concentrations of CsDPA; the other four spectra were obtained at such low concentrations that the absorption of the higher aggregate was negligible. The calculated equilibrium constants did not show any systematic variation with the formal concentration but varied randomly.

The spectroscopic data collected at −15 °C were similarly treated, and assuming a monomer/dimer equilibrium, K_2 was found to be 269 ± 4 M^{-1}, in accord with the results from the acidity data.

Conductivity. Figure 4 shows a plot of the limiting conductance (Λ_c) against concentration for LiDPA in THF at 25.00 ± 0.04 °C, and at the lower concentrations, the conductance appears to be due to free ions, thus obeying the Ostwald dilution law. The increase in the conductance at higher concentrations is generally attributed to the formation of triple ions and/or higher aggregates which are considered to be more mobile than the heavily solvated single ions.[18] The conductivity of LiDPA is only slightly greater than the background conductivity, but a crude estimate of the dissociation constant K_d can be obtained using the method of Kraus and Bray:[19]

$$K_d = c(\Lambda_c/\Lambda_o)^2$$

where c is the molar concentration, Λ_c is the equivalent conductance (cm^2 Ω^{-1} mol^{-1}) at concentration c, and Λ_o is the limiting equivalent conductance which is calculated[13b] to be 85 cm^2 Ω^{-1} mol^{-1}. Using only the data to the left of the minimum in Figure 4, K_d is (5 ± 4) × 10^{-12} M. Although this value is only approximate (order of magnitude), it does show that K_d is very small. For comparison, dissociation constants for cesium and lithium salts of fluorene derivatives in THF are typically on the order of 10^{-8} M^{-1} and 10^{-5} M^{-1}, respectively.[13b]

Discussion

Various methods have been used in the study of the aggregation of alkali amides in solution. Colligative property measurements[14,20] yield average aggregation numbers, but the unambiguous determination of the aggregates that are actually present in solution is generally not possible. However, it has recently been shown that such determinations are sometimes possible when the solvent is noncoordinating.[21] NMR spectroscopy is a powerful tool in elucidating structures of aggregates,[6,14,20,22] and even the degree of coordination of the solvent or additive to the lithium cation can be determined in favorable cases. NMR suffers from the disadvantage that its time scale can be slow with respect to chemical processes (such as exchange). All of these methods are well-suited for the study of rather concentrated solutions (about 10^{-2} M and higher), but we desire a method that is practicable for the dilute solutions that we typically employ (10^{-3}–10^{-5} M). We have previously shown that ion-pair acidity studies do give average aggregation numbers in dilute solution[17,23] but the determination of equilibrium constants among aggregates is possible only by assuming which species are present.[23a] In this paper, we show that a slightly different analysis of ion-pair acidity data coupled with a spectroscopic analysis can provide evidence regarding the aggregates that are actually present in solution, without making such assumptions. Although we apply the theory to a system that gives monomers and dimers, the theory is general for any number of aggregates. Furthermore, the monomeric species need not be present, despite eqs 2 and 3.

The methods discussed in the Results section yield aggregation constants (eq 3) based on hypothetical aggregation models. Alone, neither of the methods is capable of ruling out any of the assumed models, but the derived equilibrium constants agree (within 2 standard deviations) only under the assumption of a monomer/

(18) (a) Beronius, P.; Lindbäck, T. *Acta Chem. Scand.* **1978**, *A32*, 423. (b) Beronius, P.; Lindbäck, T. *Acta Chem. Scand.* **1979**, *A33*, 397. (c) DePalma, V. M.; Arnett, E. M. *J. Am. Chem. Soc.* **1978**, *100*, 3514.

(19) (a) Kraus, C. A.; Bray, W. C. *J. Am. Chem. Soc.* **1913**, *35*, 1315. (b) Streitwieser, A., Jr.; Padgett, W. M., III; Schwager, I. *J. Phys. Chem.* **1964**, *68*, 2922.

(20) For cryoscopic and NMR measurements of amide solutions, see: (a) Armstrong, D. R.; Barr, D.; Clegg, W.; Hodgson, S. M.; Mulvey, R. E.; Reed, D.; Snaith, R.; Wright, D. S. *J. Am. Chem. Soc.* **1989**, *111*, 4719. (b) Barr, D.; Clegg, W.; Hodgson, S. M.; Lamming, G. R.; Mulvey, R. E.; Scott, A. J.; Snaith, R.; Wright, D. S. *Angew. Chem., Int. Ed. Engl.* **1989**, *28*, 1241. (c) Armstrong, D. R.; Mulvey, R. E.; Walker, G. T.; Barr, D.; Snaith, R.; Clegg, W.; Reed, D. *J. Chem. Soc., Dalton Trans.* **1988**, 617. (d) Kallman, N.; Collum, D. B. *J. Am. Chem. Soc.* **1987**, *109*, 7466. (e) Barr, D.; Snaith, R.; Wright, D. S.; Mulvey, R. E.; Jeffrey, K.; Reed, D. *J. Organomet. Chem.* **1987**, *325*, C1. (f) Wanat, R. A.; Collum, D. B.; Van Duyne, G.; Clardy, J.; DePue, R. T. *J. Am. Chem. Soc.* **1986**, *108*, 3415. (g) Reed, D.; Barr, D.; Mulvey, R. E.; Snaith, R. *J. Chem. Soc., Dalton Trans.* **1986**, 557. (h) Armstrong, D. R.; Barr, D.; Clegg, W.; Mulvey, R. E.; Reed, D.; Snaith, R.; Wade, K. *J. Chem. Soc., Chem. Commun.* **1986**, 869. (i) Seebach, D.; Bauer, W.; Hansen, J.; Laube, T.; Schweizer, W. B.; Dunitz, J. D. *J. Chem. Soc., Chem. Commun.* **1984**, 853.

(21) Davidson, M. G.; Snaith, R.; Stalke, D.; Wright, D. S. *J. Org. Chem.* **1993**, *58*, 2810.

(22) (a) Gilchrist, J. H.; Harrison, A. T.; Fuller, D. J.; Collum, D. B. *J. Am. Chem. Soc.* **1990**, *112*, 4069. (b) Jackman, L. M.; Scarmoutzos, L. M.; Porter, W. *J. Am. Chem. Soc.* **1987**, *109*, 6524. (c) Jackman, L. M.; Scarmoutzos, L. M. *J. Am. Chem. Soc.* **1987**, *109*, 5348. (d) Jackman, L. M.; Scarmoutzos, L. M.; Smith, B. D.; Williard, P. G. *J. Am. Chem. Soc.* **1987**, *109*, 6058. (e) Galiano-Roth, A. S.; Michaelides, E. M.; Collum, D. B. *J. Am. Chem. Soc.* **1988**, *110*, 2658.

(23) (a) Ciula, J. C.; Streitwieser, A. *J. Org. Chem.* **1992**, *57*, 431. (b) Krom, J. A.; Streitwieser, A. *J. Am. Chem. Soc.* **1992**, *114*, 8747.

dimer equilibrium (Tables III and IV). The monomer/trimer and monomer/tetramer models give K_n values that differ between the two methods by more than a factor of 5 and 10, respectively; these discrepancies are well outside the estimated uncertainties. Presumably, the assumption of higher aggregates would give results that are in even poorer agreement. We can therefore conclude with a high degree of confidence that, at the concentrations in these experiments, CsDPA in THF at 25 °C is essentially a mixture of monomeric (λ_{max} = 369.5 nm) and dimeric (λ_{max} = 352 nm) ion-pair aggregates, with dimerization constant $K_2 = 160 \pm 10$ M^{-1} (obtained as an average of the results of the two methods). This conclusion is supported by the observation of dimeric cesiocarbazole in the crystalline state.[12a] Other aggregates either do not contribute significantly to the observed spectra or have absorption envelopes that are not much different from those of the major species, but their possible presence in low concentration might account for the slight discrepancies between the two methods.

From the results of method A, the equilibrium constant for eq 1b at 25 °C is 1.54, giving 24.20 for the cesium ion-pair acidity of diphenylamide (DPA). Comparison of this result with the free ion acidity in DMSO[24] (pK = 24.95) indicates that the CsDPA ion pair in THF is slightly stabilized relative to the highly delocalized fluorenyl-type ion pairs; the lower pK of 22.94 in aqueous DMSO[25] is probably a consequence of preferential stabilization of the DPA anion by hydrogen bonding.[24] Results obtained at −15 °C give K = 1.21 for eq 1b. The thermodynamic parameters are therefore $\Delta H°$ = 1 kcal/mol and $\Delta S°$ = 4 eu. These results are approximate because data have been obtained only at two temperatures; the uncertainties are probably about 0.5 kcal/mol and 2 eu, respectively.[26,27]

The lithium ion-pair acidity data show that LiDPA is a monomeric ion pair, in agreement with Collum's NMR results.[14] The lithium ion-pair pK of DPA is found to be 19.05. From the ion-pair acidity data and the known[13b] dissociation constants of LiPhFL and CsPhFL, simple algebra shows that the dissociation constant of monomeric CsDPA is 200–300 times greater than that of LiDPA, that is, LiDPA is a "tighter" ion pair than is CsDPA. The conductivity data for LiDPA shows that its dissociation constant is on the order of 10^{-12}–10^{-11} M. This dissociation constant is about 7 orders of magnitude smaller than those of lithiated fluorene derivatives,[13b] which are known to exist, generally, as solvent-separated ion pairs in THF,[16,28] suggesting that LiDPA is a contact ion pair. By a simple electrostatic argument,[28a,29] the fact that the λ_{max} of LiDPA is at a shorter wavelength than that of monomeric CsDPA provides support for this hypothesis. Additional support is provided by Velthorst's studies in which he found that the lithium and potassium salts of carbazole, indole, and 4,5-iminophenanthrene form contact ion pairs in THF.[30] Because of the proximity of two cations in the dimer as opposed to one in the monomer, similar reasoning predicts that the λ_{max} of dimeric CsDPA should be shorter than that of monomeric CsDPA, as is observed.

The thermodynamic parameters for the ion-pair dimerization of CsDPA (eq 2 with n = 2) are $\Delta H°$ = −2 kcal/mol and $\Delta S°$ = 4 eu. The observation that CsDPA has a greater tendency to aggregate compared to LiDPA is not unexpected. It has been found in other systems[5,31] that the dimerization of lithiated species is an endothermic but entropically favorable process, indicating the stronger specific solvation of the lithium ion in the monomer. Furthermore, conductivity experiments suggest that the cesium ion is not specifically coordinated to THF.[28b] Thus, there should be less inhibition to dimerization (which, in the absence of solvent, is probably favorable because of coulombic interactions) in the case of the cesium ion pair. Nevertheless, the fact that the magnitude of the entropy of dimerization is not large and is negative (−20 to −40 eu) shows that the monomer is more highly solvated than the dimer.

Conclusions

LiDPA exists as a monomeric contact ion pair in THF solution at 25 °C. The ion-pair pK of DPA on the previously defined lithium scale[13b,16] is 19.05, and the dissociation constant of its lithium ion pair to free ions is about 10^{-12}–10^{-11} M. CsDPA exists as monomer and dimer in THF solution with dimerization constant $K_2 = 160 \pm 10$ M^{-1} at 25 °C and $K_2 = 270 \pm 40$ M^{-1} at −15 °C ($\Delta H°$ = −2 kcal/mol, $\Delta S°$ = 4 eu). The ion-pair pK on the previously defined cesium scale[13] is 24.20. A new method is presented for the determination of aggregation constants in dilute solution on the basis of an analysis of spectroscopic changes with concentration. Even though the change in λ_{max} is small and the amount of dimer in the most concentrated solution is only 10%, this method is shown to provide unique information about the nature of the aggregate and aggregation equilibrium constants of reasonable precision.

Experimental Section

General. Ion-pair acidity and spectral studies were carried out in a Vacuum/Atmospheres glovebox under an argon atmosphere. The UV–visible absorption spectra were obtained on a computer-driven Shimadzu Model UV-2101PC spectrophotometer custom fitted with fiber-optic cables. In order to allow spectral studies to be carried out under the inert atmosphere of the glovebox, the optical cables were connected as follows. A thermostatted cell block for the UV cells was fitted with aligned mounts for the optical cables, and the cell block was placed in an aluminum well. The ends of the optical cables were routed through holes in the sides of the well and connected to the mounts. The holes were sealed, and the well was attached to the bottom of the glovebox. The other ends of the optical cables were then connected to the spectrophotometer.

Details of the conductivity apparatus have been previously published.[13b]

All of the absorption spectra were scanned at a rate of 200 nm/min at 0.5-nm intervals using a 2-nm slit width.

Computations were generally carried out using double-precision floating-point arithmetic (52 bit precision). The FORTRAN algorithm for the singular-value decomposition (SVD) was implemented as published.[15b]

Diphenylamine (DPA). An ethyl ether solution of commercial material (MCB) was washed three times with 10% aqueous NaOH and dried over anhydrous $MgSO_4$. The solvent was removed by rotary evaporation, and the solid was recrystallized three times from hexane and sublimed under vacuum (10^{-2} mmHg) at 55 °C. The entire sublimation apparatus was taken into the glovebox to avoid exposing the DPA to air; mp = 55.8–57.0 °C (lit.[32] mp = 54–55 °C). Further evidence of purity was provided by the NMR spectrum.

Molecular Sieves. A Schlenk flask containing Linde 3A molecular sieves was placed on the vacuum line and heated to about 200 °C for 1 or 2 d until the pressure returned to its initial value (about 10^{-2} mmHg) as indicated by the pressure gauge. The stopcock was closed, and the

(24) Bordwell, F. G.; Algrim, D. J. *J. Am. Chem. Soc.* **1988**, *110*, 2964.
(25) Cox, R. A.; Stewart, R. *J. Am. Chem. Soc.* **1976**, *98*, 488.
(26) The acidities of a series of aniline derivatives have been determined in ammonia solvent. See: (a) Birchall, T.; Jolly, W. L. *J. Am. Chem. Soc.* **1966**, *88*, 5439. (b) Takemoto, J. H.; Lagowski, J. J. *Inorg. Nucl. Chem. Lett.* **1970**, *6*, 315. (c) Lagowski, J. J. *Pure Appl. Chem.* **1971**, *25*, 429.
(27) For acidities of amines in THF, see: (a) Ahlbrecht, H.; Schneider, G. *Tetrahedron* **1986**, *42*, 4729. (b) Fraser, R. R.; Mansour, T. S. *J. Org. Chem.* **1984**, *49*, 3442. (c) Denniston, A. D. Ph.D. Dissertation, University of Washington, 1979.
(28) (a) Hogen-Esch, T. E.; Smid, J. *J. Am. Chem. Soc.* **1966**, *88*, 307. (b) Hogen-Esch, T. E.; Smid, J. *J. Am. Chem. Soc.* **1966**, *88*, 318.
(29) (a) Carter, H. V.; McClelland, B. J.; Warhurst, E. *Trans. Faraday Soc.* **1960**, *56*, 455. (b) Hoijtink, G. J. *Ind. Chim. Belge* **1963**, *12*, 1371. (c) Buschow, K. H. J.; Hoijtink, G. J. *J. Chem. Phys.* **1964**, *40*, 2501. (d) Buschow, K. H. J.; Dieleman, J.; Hoijtink, G. J. *J. Chem. Phys.* **1965**, *42*, 1993. (e) Velthorst, N. H.; Hoijtink, G. J. *J. Am. Chem. Soc.* **1965**, *87*, 4529.
(30) (a) Velthorst, N. H. *Pure Appl. Chem.* **1979**, *51*, 85. (b) Vos, H. W.; Blom, H. H.; Velthorst, N. H.; MacLean, C. *J. Chem. Soc., Perkin Trans. 2* **1972**, 635.
(31) (a) Fraenkel, G.; Chow, A.; Winchester, W. R. *J. Am. Chem. Soc.* **1990**, *112*, 6190. (b) McGarrity, J. F.; Ogle, C. A. *J. Am. Chem. Soc.* **1984**, *107*, 1805. (c) Seebach, D.; Hässig, R.; Gabriel, J. *Helv. Chim. Acta* **1983**, *66*, 308.
(32) Brown, W. G.; Kharasch, M. S.; Sprowls, W. R. *J. Org. Chem.* **1939**, *4*, 442.

flask was allowed to cool and taken into the glovebox without exposing the sieves to air.

Tetrahydrofuran (THF). Commercial material (Fisher) was distilled from sodium/benzophenone or from lithium aluminum hydride, degassed, stirred over sodium–potassium alloy until the characteristic blue color appeared, and vacuum-transferred into a flame-dried receiver. The solvent was taken into the glovebox and stored over activated Linde 3A molecular sieves. The THF was allowed to stand over the sieves for about 1 week before use. The THF prepared in this way typically contained about 10^{-4} M water, as determined by the quenching of the reaction of a THF solution of (diphenylmethyl)cesium.

(Diphenylmethyl)cesium (CsDPM). Commercial (Aldrich) diphenylmethane was recrystallized several times from 95% ethanol, sublimed under vacuum, and taken into the glovebox. Commercial cesium metal (Aldrich or Dow) was taken into the glovebox without further purification. In the glovebox, about 200 mg of diphenylmethane was added to about 130 mg of cesium in 5 mL of THF. The mixture immediately turned dark orange and evolved a gas (presumably hydrogen). The mixture was allowed to stand overnight. Complete reaction was indicated by the total consumption of the metal and the cessation of gas evolution. Stock solutions prepared in this way were stable for at least a few weeks in the glovebox.

Absorption Spectra of Cesium Diphenylamide (CsDPA) in THF. The spectra were obtained over the wavelength range of 340.0–450.0 nm; DPA does not absorb in this region of the spectrum. A solution of about 2 mg of DPA in about 1.5 mL of THF was prepared in a UV cell, and the base-line spectrum was obtained. Aliquots of a stock solution of CsDPM were added via microsyringe to the solution, and the absorption spectrum was obtained after each addition. A total of 12 spectra were obtained and processed by SVD.

Extinction Coefficient of Cesium Diphenylamide (CsDPA). A stock solution of 2.877 mg of DPA in 6.999 g of THF was prepared in the glovebox. An aliquot of this solution was added to each of five UV cells containing known masses of THF; the mass of the aliquot was then determined by difference. In this manner, five solutions varying in known concentration from 8.82×10^{-5} to 4.63×10^{-4} M DPA were prepared. The manipulations were carried out as rapidly as possible in order to minimize the change in concentration of the stock solution because of evaporation of the solvent. Aliquots of a stock solution of CsDPM were added to each of the solutions in the UV cells until the absorption band of CsDPM persisted. The spectrum of each of the solutions was deconvoluted by a least-squares fitting procedure using the separate spectrum of CsDPM and the SVD basis (U_1 and U_2; see the Results section) for the spectrum of CsDPA; this treatment effectively subtracts the absorbance band of the CsDPM from the original spectrum, leaving only the absorbance band of CsDPA. Because CsDPM is basic enough to essentially completely deprotonate the DPA, the extinction coefficient of the CsDPA was then calculated directly.

Ion-Pair Acidity Studies. For the acidity studies, absorption spectra were obtained over the wavelength range of 340–700 nm. Preliminary experiments showed that 9-*tert*-butylfluorene (9-*t*-BuFL) is an appropriate indicator for the determination of the acidity of DPA. In a typical experiment, known quantities (2–20 mg) of DPA and 9-*t*-BuFL were added to a known amount (1–2 g) of THF in a UV cell to give a solution of known initial concentration of the "neutrals"; the base-line spectrum was obtained. To the solution was added an aliquot of a stock solution of CsDPM via microsyringe. The mixture was shaken and allowed to stand for about 3–5 min in the thermostatted cell block (25.0 °C) until the absorption spectrum was stable, and the spectrum of the equilibrated mixture was obtained. Another aliquot of CsDPM was added to the cell, and the procedure was repeated. In this manner, several equilibrations at differing concentrations of the ion pairs were obtained from a single cell. The entire procedure was repeated for a total of 19 equilibria from three experimentally independent cells. The spectra of the equilibrium runs were deconvoluted as for the extinction coefficient determinations; from the known extinction coefficient of Cs-9-*t*-BuFL and that of CsDPA determined in this work, the formal concentrations of the ion pairs were determined directly, and the concentrations of the neutrals were determined by difference from their known initial concentrations.

The lithium ion-pair acidity was determined in a similar fashion, but the spectral deconvolution was simplified because of the constant shape of the absorption spectrum.

Error Analysis. Because our interpretation relies on a significance test, it is appropriate to give an outline of our methods of uncertainty estimation. All of the stated uncertainties are ±1 standard deviation. We took into account both random and systematic errors.

The given uncertainty in the observed extinction coefficient of LiDPA and CsDPA is simply the standard deviation calculated from three and five determinations, respectively.

Method A. For a single equilibrium experiment, most of the random component of the uncertainty arises from the noise of the spectrophotometer; errors in weighing are negligible in comparison. However, for a series of experiments, as in the present case, it is more difficult to take into account the uncertainty in the pathlength of the UV cell, which is about 0.01 mm. For a series of spectra obtained from the same cell, this error is systematic, but from cell to cell it is random. Therefore, the contributions of all of the random errors to the uncertainties in Table II were estimated as follows. Each data point was assigned an identical weight, and the best fit to eq 4 was calculated. The standard deviation σ of the ordinate values was calculated assuming no error in the abscissa values; this standard deviation was then used to assign the statistical weights ($1/\sigma^2$ for both variables) in the original data, and the best fit was recalculated. Note that finding the standard deviation of the data points in this manner assumes that the model to be fit to the data is the correct one, so that there is no independent test for goodness-of-fit. This treatment should overestimate somewhat the actual uncertainties in the variables and, consequently, in the calculated parameters. The uncertainties in the extinction coefficients of the ion pairs are systematic errors for this method; their effects were determined by direct recalculation of the quantities of interest (Table II) when variable was replaced by variable ± uncertainty. Finally, the total estimated uncertainty in the best-fit parameters was found by summation in quadrature of the random and systematic errors. The contribution of the uncertainty in the extinction coefficient of Cs-*t*-BuFL to the uncertainty in the K_ns canceled exactly when the latter quantity was calculated from the parameters.

Method B. Almost all of the uncertainty in the calculated extinction coefficients of the aggregates derives from the uncertainty in the value of the observed extinction coefficient, which is a systematic error in eq 10. The random component of the uncertainties in the aggregation constants is determined from the scatter about the average value calculated from the spectra obtained at the eight highest concentrations. The systematic component was directly calculated by direct substitution, as in the analysis for method A. Finally, the total uncertainties in the aggregation constants were calculated from summation in quadrature of the systematic and random errors.

Acknowledgment. This work was supported in part by NIH Grant GM 30369.

Appendix. Spectroscopic Analysis (Method B)

In this method, we make use of the results of the SVD analysis of the spectral data. The goal is to transform the matrices (**US**) and $\mathbf{V}^t$ into matrices that have direct chemical significance: we wish to find a matrix, **Q**, whose column vectors correspond to chemically meaningful spectra of the various aggregates in solution. Necessarily, these vectors form a basis for the column space of the original (experimental) matrix **B** (see Results section). Since our original spectral data (columns of **B**) were obtained as a function of the total concentration, we have $\mathbf{B} = \mathbf{QP}$, where the columns of **Q** are actual spectra of the aggregates and **P** somehow depends on the concentration.

Consider the observed absorbance at a fixed wavelength, A_λ. Assuming that the absorbances of all of the aggregates obey Beer's law, we have with eq 3

$$A_\lambda = \sum_n \epsilon_{\lambda n}[(\mathrm{CsDPA})_n] = \sum_n \epsilon_{\lambda n} K_n [(\mathrm{CsDPA})_1]^n \quad (6)$$

where $\epsilon_{\lambda n}$ is the extinction coefficient at wavelength λ of the aggregate composed of n ion pairs. For simplicity, the pathlength of the cell has been incorporated into A_λ. A_λ is an entry of the matrix **B**; writing eq 6 in terms of matrix multiplication, we therefore have

$$\mathbf{B} = \begin{matrix} \epsilon_{11} & \epsilon_{12}K_2 & \epsilon_{13}K_3 & \cdots & \epsilon_{1N}K_N \\ \epsilon_{21} & \epsilon_{22}K_2 & \epsilon_{23}K_3 & \cdots & \epsilon_{2N}K_N \\ \vdots & \vdots & \vdots & & \vdots \\ \epsilon_{M1} & \epsilon_{M2}K_2 & \epsilon_{M3}K_3 & \cdots & \epsilon_{MN}K_N \end{matrix} \times \begin{matrix} c_1 & c_2 & c_3 & \cdots \\ c_1^2 & c_2^2 & c_3^2 & \cdots \\ \vdots & \vdots & \vdots & \\ c_1^N & c_2^N & c_3^N & \cdots \end{matrix} \quad (7)$$

where M is the number of discrete wavelengths in the spectra, N is the degree of the largest aggregate, and c_i is the concentration of the *monomeric* CsDPA in the ith experiment; in practice, some of the Ks will generally be set to zero under a given hypothesis. The number of columns in the right-hand matrix is equal to the number of experimental spectra. The difficulty is that c_i is an unknown quantity, so all of the elements of the c matrix are unknown. However, we can transform the c matrix into a useful form by the following device: we write the concentration of the monomer in the ith experiment as a fraction, f_i, of the concentration in the first experiment, and we then have

$$\begin{matrix} c_1 & c_2 & c_3 & \cdots \\ c_1^2 & c_2^2 & c_3^2 & \cdots \\ \vdots & \vdots & \vdots & \\ c_1^N & c_2^N & c_3^N & \cdots \end{matrix} = \begin{matrix} c_1 & f_2c_1 & f_3c_1 & \cdots \\ c_1^2 & f_2^2c_1^2 & f_3^2c_1^2 & \cdots \\ \vdots & \vdots & \vdots & \\ c_1^N & f_2^Nc_1^N & f_3^Nc_1^N & \cdots \end{matrix}$$

Equation 7 can now be rewritten as

$$\mathbf{B} = \begin{matrix} \epsilon_{11}c_1 & \epsilon_{12}K_2c_1^2 & \epsilon_{13}K_3c_1^3 & \cdots & \epsilon_{1N}K_Nc_1^N \\ \epsilon_{21}c_1 & \epsilon_{22}K_2c_1^2 & \epsilon_{23}K_3c_1^3 & \cdots & \epsilon_{2N}K_Nc_1^N \\ \vdots & \vdots & \vdots & & \vdots \\ \epsilon_{M1}c_1 & \epsilon_{M2}K_2c_1^2 & \epsilon_{M3}K_3c_1^3 & \cdots & \epsilon_{MN}K_Nc_1^N \end{matrix} \times \begin{matrix} 1 & f_2 & f_3 & \cdots \\ 1 & f_2^2 & f_3^2 & \cdots \\ \vdots & \vdots & \vdots & \\ 1 & f_2^N & f_3^N & \cdots \end{matrix} \quad (8)$$

The matrices in eq 8 are now identified with the matrices **Q** and **P**, respectively, as discussed above. It is easily seen that the columns of **Q** correspond to the spectra (i.e., extinction coefficient as a function of wavelength) of the various aggregates, each multiplied by a constant. The important point is that some of the elements (those in the first column) of **P** are known; this fact allows us to find a transformation of the SVD results into a chemically meaningful form, as we now show. We have

$$\mathbf{B} = (\mathbf{US})\mathbf{V}^t = \mathbf{QP} \quad (9)$$

Recalling that (**US**) and **Q** are both bases for the column space of **B**, there must be a linear transformation, **T**, such that

$$(\mathbf{US})\mathbf{T} = \mathbf{Q} \quad (10)$$

With $\mathbf{T}(\mathbf{T}^{-1}) = 1$, from eq 9, we have $\mathbf{T}^{-1}\mathbf{V}^t = \mathbf{P}$. Since the form of **P** is known (eq 8), the elements of $\mathbf{T}^{-2}$ can be found by nonlinear least squares if the number of experimental spectra exceeds the number of nonzero rows of **P**. Finally, **Q** is computed according to eq 10. In practice, the computed matrix **P** does not have the exact form indicated in eq 8 but best approximates that form in a least-squares sense. Furthermore, the results depend on the signal-to-noise ratio of the first input spectrum because the elements in the first column of **P** are set to unity; therefore, we always choose the spectrum with the highest signal-to-noise ratio as the first column of **B**.

In order to calculate the equilibrium constants among the various aggregates, we use the observed extinction coefficient at a given wavelength. In the present case, it is convenient to use 367 nm because the observed extinction coefficient was found experimentally to be independent of the formal concentration at that wavelength. With the first summation in eq 2, we have, at a fixed wavelength

$$A_{ob}/\epsilon_{ob} = \{\text{CsDPA}\} = \sum_n nA_n/\epsilon_n \quad (11)$$

where A_{ob} and ϵ_{ob} are the observed absorbance and extinction coefficient, respectively, and A_n and ϵ_n are the absorbance and extinction coefficient of the nth aggregate, respectively. We have again assumed that the absorbances of all species obey Beer's law. Using the same data from the spectral analysis, the A_ns are given directly from the matrices **Q** and **P** above: for the ith spectrum at wavelength λ, $A_n = \mathbf{Q}_{\lambda n}\mathbf{P}_{ni}$. We therefore have a system of several equations in the unknowns ϵ_n that can be solved by straightforward least-squares fit to eq 11. Finally, the concentrations are calculated according to Beer's law, and the K_ns are found according to eq 3.